

***Copyright 1996 Society of Photo-Optical Instrumentation Engineers.**

This paper was published in the Proceedings of SPIE Microwave Sensing and Synthetic Aperture Radar, 23 September 1996, Taormina (Italy) and is made available as an electronic reprint with permission of SPIE.

One print or electronic copy may be made for personal use only. Systematic or multiple reproduction, distribution to multiple locations via electronic or other means, duplication of any material in this paper for a fee or for commercial purposes or modification of the content of the paper are prohibited

Developments in Satellite Radar Altimetry

C. Zelli*, F. Impagnatiello*

G. Alberti**

*Alenia Spazio S.p.A.

Remote Sensing Group Via Saccomuro, 24 - 00131 Rome (Italy)

**CO.R.I.S.T.A. consortium

P.le Tecchio, 80 - 80125 Naples (Italy)

ABSTRACT

This paper briefly overviews the status of the research in the development of new altimeter systems presently carried out in Alenia Spazio S.p.A. in the frame of internal research activities and European Space Agency (ESA) feasibility study contracts.

In particular, the concepts of synthetic aperture and interferometric altimetry for global ice/land topography are reviewed in this paper. These system designs are extremely promising, since they can overcome the limitations of the classic nadir-looking pulse limited systems. Conventional systems in fact, in spite of the extremely high range accuracy achievable over oceans, are unable to provide topographic details over ice or land due to their coarse horizontal resolution, several hundreds of meters against the 100 - 300 m required in ice/land topography applications.

Keywords: altimetry, deramping, interferometry, Earth topography, synthetic aperture radar.

1. INTRODUCTION

Radar altimeters designed up to now (Seasat, Geosat, ERS-1/2, Topex/Poseidon) have widely demonstrated the capability of performing measurements of the ocean topography from space with a high degree of accuracy. Nevertheless none of the mentioned systems provides an extensive capability to get topographic measurements over ice and land surfaces as requested by scientists.

An improvement in this area will be possible with RA-2¹, Advanced Radar Altimeter for ENVISAT-1 mission, currently under development in Alenia Spazio, thanks to its special on board tracker design but novel concepts have to be developed to meet the severe horizontal resolution requirements (order of 100 - 300 meters vs. the several hundred meters provided by nadir-looking pulse limited systems) typical of ice/land topography missions.

To obtain high resolution measurements over large swath different systems based either on multi-beam² and multi-antenna³ configurations or on synthetic aperture processing applied to altimetric systems have been proposed by various authors^{4,5,6,7} in the technical literature and the concept of synthetic aperture particularly looks as a very interesting option to enhance the horizontal resolution in the direction of satellite motion.

As a matter of fact, Alenia Spazio is studying in depth the possibility of applying the synthetic aperture concept to radar altimetry for global Earth topography missions and is further moving towards the applicability of interferometry at very low off-nadir angles for the bidimensional retrieval of height measurements within the observed system swath. This is a really innovative measurement technique respect to conventional interferometry⁸ because thanks to the particular observation geometry and baseline selection a unique interference fringe can be generated within the observed swath thus avoiding the troubles of phase unwrapping otherwise required in conventional interferometric processing.

In the following the preliminary design results regarding power budgets, on-board processing requirements and performance evaluation for a Ka band (37 Ghz), a Ku band (13.6 Ghz) nadir looking synthetic aperture and a Ku band near sub-nadir interferometric altimeters are reported.

2. SYNTHETIC APERTURE RADAR ALTIMETER

2.1 Review of key concepts

The technique for synthesising a large antenna through radar motion is well established for side-looking systems. Such systems are able to produce high resolution images by exploiting the doppler shift caused by the relative motion between the radar and the imaged surface; the final effect can be viewed as a remarkable reduction of the antenna aperture in the direction of motion (along track). This basic principle is certainly applicable to radar altimeters, taking into account the differences between instruments, mainly in terms of required resolution and application.

The doppler effect is a frequency shift measured in the received signal due to the distance variation between source and target. Therefore, the signal coming from a single point target presents a time varying frequency, covering a frequency band whose width depends on the time interval T within which the target is observed. Greater the so called integration time T is, wider the signal band will result. The upper limit for the values of T is imposed by the received signal power which, through the attenuation introduced by the antenna pattern, determines the useful frequency band and, consequently, the spatial resolution attainable by the system.

By using the -3dB band definition, the well known theoretical resolution (r) for synthetic aperture radar systems can be approximated as:

$$r \approx \frac{\lambda R_0}{2vT} = \frac{\lambda}{2\vartheta_3} \quad (1)$$

where λ is the wavelength, v is the platform velocity, R_0 is the minimum radar-target distance and ϑ_3 is the -3 dB antenna aperture. In other words, by exploiting the frequency band caused by the doppler effect, the system is able to "synthesise" a very large antenna in the sense that it is able to attain a spatial resolution which would have been reached by a conventional radar but with a very narrow beam ϑ_{sth} given by:

$$\vartheta_{\text{sth}} = \frac{r}{R_0} \approx \frac{\lambda}{2vT_i} \approx \frac{\lambda}{2\vartheta_3 R_0} \quad (2)$$

In this way, resolutions of few meters can be reached, but quite sophisticated data processing is in principle required, because the phase variation introduced by the doppler effect should be compensated through complex filters which, in addition, are intrinsically bidimensional. Instead, a synthetic aperture radar altimeter should be able to perform data processing in real time on board and, moreover, resolutions such those attainable with accurate bidimensional processing are absolutely not needed.

In this case an unfocused processing can be used if phase variation along a synthetic aperture is maintained sufficiently low (below 0.25π), significantly simplifying the required data processing. The resulting integration time (T_u) and attainable resolution r_u , which are function only of the wavelength and the spacecraft altitude h , are then given by:

$$T_u = \frac{2}{v} \sqrt{\frac{\lambda h}{8}}, \quad r_u = \sqrt{\frac{h \lambda}{2}} \quad (3)$$

2.2 - Expected average return waveform and signal to noise ratio evaluation

Conventional radar altimeters operate in pulse-limited mode, since their instantaneous area of illumination is directly proportional to the compressed pulse length. In this case the average return can be evaluated analytically⁹. When a synthetic aperture processing is applied, the resulting antenna pattern sharpening along the spacecraft velocity direction allows the system to work in a beam-limited condition in along track. In this case, the received waveform $P_r(\tau)$ can be approximated with the following gaussian shape, function of the time delay τ relative to the pulse transmission instant:

$$P_r \approx \frac{E \lambda^2 G_0^2 \bar{\sigma}^0}{64 \log 2 \pi G \sigma_c \sqrt{2 \log 2}} \frac{\vartheta_{3x} \vartheta_{3y}}{h^2} \exp \left[\frac{F}{G} \frac{\tau^2}{2 \sigma_c^2} \right] \quad (4)$$

E is the transmitted energy per pulse, G_0 is the maximum antenna gain, $\bar{\sigma}^0$ is the mean backscattering coefficient of the illuminated area, ϑ_{3x} is the synthesised antenna aperture in the along-track direction, ϑ_{3y} is the real antenna aperture in the across-track direction and σ_c depends on both system bandwidth B and surface height r.m.s. through the following equation:

$$\sigma_c = \sqrt{\frac{1}{8 \log 2 B^2} + \frac{F \sigma_s^2}{G_c k}} \quad (5)$$

Expression (4) can be used to evaluate the expected peak value of the signal to noise ratio (SNR) which represents one of the most important parameters affecting the final system performance. By dividing the peak value of (4) by the thermal noise power and the various loss sources, it is possible to derive the following expression for the signal to noise ratio, where it is worth underlining the dependence on the inverse of the altitude squared and the contribution of the number of pulses (N_p) coherently summed during the integration time:

$$\text{SNR} = \frac{E N_p \bar{\sigma}^0}{64 \log 2 \sigma_c \sqrt{2 \log 2}} \eta_a^2 \frac{E D_x D_y}{G \lambda} \frac{I^2}{k} \frac{\vartheta_{3x} \vartheta_{3y}}{h^2} \frac{1}{k T_0 B F} \frac{1}{L_{RF} L_a} \quad (6)$$

where $k T_0 B F$ is the thermal noise power, being k the Boltzman constant, F the receiver noise figure and T_0 the system noise temperature, L_{RF} are the total radio-frequency system losses, L_a are the two way atmospheric losses, η_a is the total antenna efficiency of D_x and D_y dimensions. The last expression can be used in the system design by setting the SNR to a value sufficient to assure a good signal detection and then by evaluating the required transmitted energy as a function of the surface height r.m.s. and backscattering coefficient.

2.3 - System timing

Being the synthetic aperture processing unfocused for the requested range of resolutions of the altimetric system (100 - 300 m), it appears convenient to operate in burst mode. This means that a certain number of pulses with a high pulse repetition frequency (PRF) are transmitted within a burst period (BRI), while the remaining time of the BRI can be exploited to receive all the returning echoes without ambiguity. The timing parameters should be designed in order to accomodate the maximum expected return time and orbit altitude variations.

The easiest and most useful way to determine the burst length is to put it equal to the processed integration time which in turn should not exceed the round trip time established by the minimal radar surface distance. Of coarse this condition puts a constraint on the effective achievable unfocused along track resolution. The PRF within the burst should also satisfy the Nyquist criterion for the doppler bandwidth sampling and its value can be determined by considering an appropriate oversampling factor and maintaining an integer number of pulses within the burst.

2.4 - Synthetic aperture altimetric processing

The new developed systems must be designed to provide both conventional and high resolution altimetric measurements through synthetic aperture processing. This means that the system should be able to work both as conventional radar altimeter and as synthetic aperture altimeter thus mantaining the compatibility with the full-deramping processing typical of any altimetric system. A conceptual block diagram of the data processing is for instance shown in figure 1.

The transmitted signals are conventional long linear frequency modulated (FM) pulses that are coherently deramped and digitally converted, maintaining the in-phase and in-quadrature (I and Q) components. A Fast Fourier Transform (FFT) is applied to the samples of each pulse in order to obtain a delay-time representation and the transformed data belonging to each

burst are recorded into a memory. Data processing is then split into two parallel branches: a conventional altimetric data processing and a synthetic aperture data processing.

The first starts by extracting, for each burst, the square modules of the samples and making an incoherent averaging over subsequent pulses in order to reduce the speckle effects. Soon after the data are processed by a robust tracker which is able to estimate the echo delay and its power. The last two information will be used to drive the chirp generator in positioning the deramping window and to set the proper attenuation in the microwave receiver to adapt its gain to the signal dynamic range. The averaged data and the estimated time delay and power are downloaded as part of the scientific data stream.

The synthetic aperture data processing is applied burst by burst and it begins with an along-track FFT, by accessing to the memory perpendicularly with respect to previously done. This operation transforms the data in a doppler-delay domain where is easy to accomplish an accurate range migration correction through a complex phase multiplication. After that, the doppler axis can be mapped in the along-track axis by exploiting the system geometry. Being the processing unfocused, the last operation is strongly simplified since each doppler bin can be mapped directly to the corresponding along-track position. In this way, a "look" of overlapping surface regions is produced for each burst and subsequent looks can be incoherently integrated to reduce the speckle. To this end, the looks should be first aligned along the cross-track direction in order to compensate possible differences in the reference time produced by the on-board tracker and later they should be shifted in the along track direction to take into account the space covered during one BRI. The final step is represented by the topography extraction from the multi-look image. In the along track direction the image is decomposed in doppler filters and each echo profile within a doppler filter can be processed⁷ through Centre of Gravity or Leading Edge Estimation algorithms to provide the height information as well as surface slope indication.

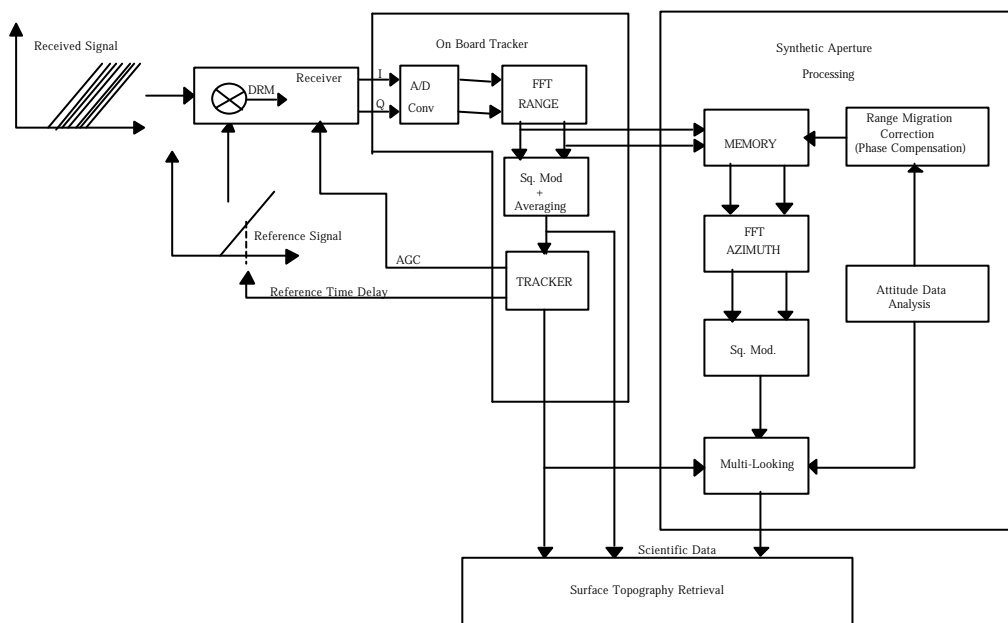


Figure 1 - Functional block diagram for combined conventional and synthetic aperture altimetric processing.

2.5 - Ka system design

The choice of a higher operating frequency respect to the typical Ku band employed in conventional pulse limited radar altimeters represents a potential solution for the resolution enhancing problem in the across-track direction. A high operative frequency in conjunction with a relatively large antenna can in fact improve by some orders of magnitude the achievable across track horizontal resolution.

Following other studies in this field⁶, a design based on the 37 GHz frequency has been considered. This choice allows to achieve a horizontal resolution of 100 m in the along-track direction by setting through (3) an integration time of about 4.35 msec and roughly 950 meters in the across track direction by considering a rectangular antenna 6 meters wide in across track (the along track size can be much shorter - order of 1 meter - being an equivalently large antenna synthesised through coherent processing in this direction) operating at 800 km altitude. Such a figure could of course be halved if a low orbit mission (400 Km altitude) is assumed in place. The across track resolution figures are not fully compliant with the topography requirements but further improvements could be gained considering a 10 meters wide antenna in the across track direction even if some technical problems (i.e. mechanical structure and deployability of the antenna) should be properly accounted for.

For the system bandwidth the choice of 50 MHz seems to be the most appropriate, because it assures a vertical resolution (3 m) in compliance with typical land/ice topography requirements. More sophisticated designs based on resolution adaptivity can however be considered; for instance, resolution switching between blocks of N consecutive synthetic apertures could be envisaged on the basis of the slope information provided in real time by the on-board conventional altimeter tracker. In this way resolution could be further decreased or improved depending on the mean surface slope. Surfaces with steep slopes, in fact, mostly require much wider range tracking windows with coarser resolution values.

Beside the vertical resolution other three key parameters have to be determined: the transmitted energy, the processed number of pulses and the along track antenna dimension. On one side the along track antenna dimension determines the attainable doppler bandwidth and, therefore, the pulse repetition frequency (PRF) needed to well sample the data. On the other side the PRF value with the established integration time enables to calculate the number of integrated pulses and to design the values of pulse duration and transmitted energy.

Operating frequency:	37 GHz	Along-track resolution:	100 m
S/C altitude:	800 Km	Integration time:	4.352 msec
Across-track antenna dimension:	6 m	Synthetic along-track antenna aperture:	7.2 mdeg
Across-track antenna aperture:	68.1 mdeg	Bandwidth:	50 MHz
Across-track resolution:	~ 950 m	Vertical resolution:	3 m
Along-track antenna dimension	1 m	Burst length	4.352 msec
Along-track -3 dB antenna aperture	7.135 mrad	Number of pulses within the burst	68
Antenna dwell time	0.766 sec	PRF	15624 Hz
Along-track -3 dB antenna aperture	7.135 mrad	BRI	13.377 msec
Doppler bandwidth	13115 Hz	Spacing between burst	~ 100 m
Spacecraft velocity	7452 m/sec	Reception length	8.96 msec
Pulse duration max.	54 µsec	Number of looks	57

Table 1 -Design parameters for the Ka system.

A good compromise would be the choice of about 1 m antenna, from which, by following the guidelines of paragraph 2.3, all the timing parameters can be determined. In particular, an oversampling factor of about 1.2 was considered for the PRF, the maximum value of pulse length was evaluated by considering a switching time of 10 µsec, while the number of available looks was calculated considering the available number of bursts within the -3 dB antenna dwell time. Table 1 shows the main system parameters determined.

Finally, the energy to be transmitted was evaluated through (6) by setting the signal to noise ratio at 10 dB, which is the figure usually employed to assure a good signal detection, and the other noise sources to the following figures, maintaining some safety margin: 6 dB for the receiver noise figure and the total RF losses, 3 dB for the two way atmospheric losses and 0.3 for the total antenna efficiency. Figure 2 shows needed peak transmitted energy as a function of surface height r.m.s. for

various backscattering coefficient values: a pulse duration of 50 μsec with a peak transmitted power of 12 Watt (0.6 mJ of transmitted energy) allows to have a signal to noise ratio of 10 dB for significant values of both backscattering coefficient and surface height r.m.s.

Such figures are compatible even with the conventional altimetric processing. In this case the system can be schematised neither as a pure pulse or beam limited because of the real aperture antenna size which entails a beam limited operation mode in across - track but a pulse limited operation mode in along track. The expected averaged waveform has been evaluated numerically; the results show nearly gaussian functions characterised by a decreasing maximum value with increasing surface height r.m.s. The expected peak signal to noise ratio for a single pulse has been numerically calculated and is plotted in figure 3 assuming the identified value of 0.6 mJ for the transmitted energy.

The resulting signal to noise ratio assures good elevation estimates for a very large interval of both backscattering coefficient and surface height r.m.s. values. It could sound strange that the signal to noise ratio for the synthetic aperture processing is smaller than the one obtained by a single pulse. But, at least in this case, the benefit due to the coherent integration of a certain number of pulses is compensated by the increasing equivalent scattering area by moving from a beam-limited condition towards a pulse-limited condition in the along track direction.

With respect to the timing mode, the compatibility between conventional and synthetic aperture processing can be verified by analysing the expected decorrelation among pulses. The amount of speckle reduction depends in fact not only on the number of averaged pulses but mostly on the degree of correlation among pulses, which increases with the PRF. The correlation distance in the along track direction can be easily calculated by applying the results of Van Cittert-Zernike theorem¹⁰. For the specific design proposed it can be shown that a halved PRF of 7812 Hz is able to assure decorrelated echoes for any surface height r.m.s. value. This means that only one pulse over two should effectively be taken into account in the average process of conventional altimetric processing, obtaining exactly 34 decorrelated pulses each burst

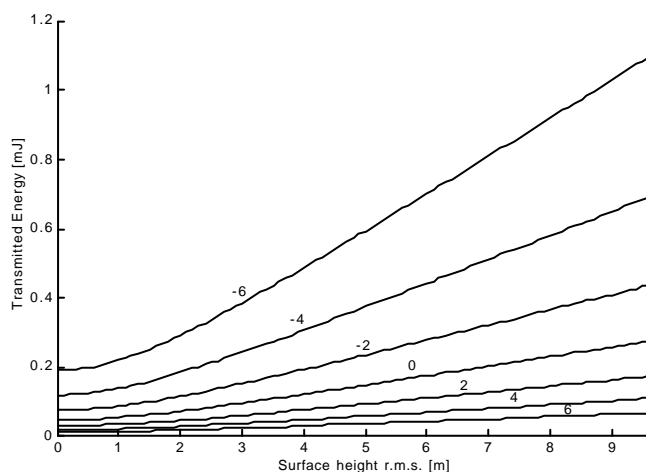


Figure 2 - Synthetic processing: transmitted energy vs surface height r.m.s. for various backscattering coefficient in dB and for a SNR of 10 dB.

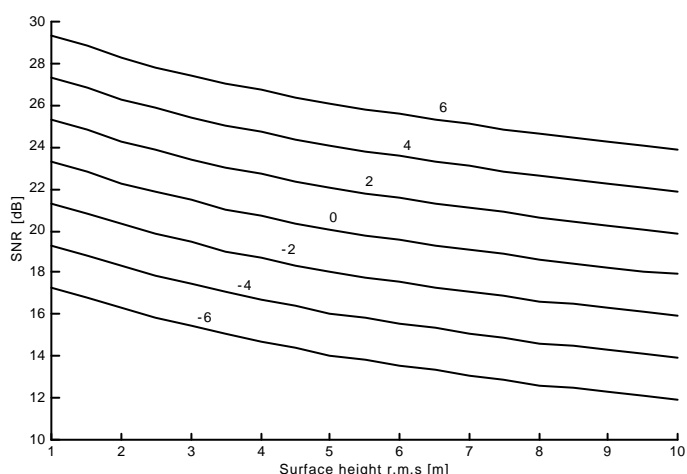


Figure 3 - Conventional altimetry: peak signal to noise ratio for a single pulse vs surface height r.m.s. for various backscattering coefficient in dB assuming transmitted energy of 0.6 mJ.

2.6 - Ku system design

The choice of Ku band allows to use more common technology at the expense of reduced resolution performance. As a matter of fact, the heritage of already developed systems like ERS-1/2 and RA-2, could be fully exploited. Therefore a 1.2 meter antenna equal to that used for the RA/2 system with the same basic hardware have been considered. Table 2 shows the main system parameters obtained following the same design procedure used for the Ka system leading to a really cost effective design fully compatible with the conventional Ku pulse limited altimeter for ocean topography measurements.

The main difference with respect to the previous system consists in the across track antenna aperture which, in this case, entails a pulse limited operation mode in this direction. Therefore, the expected received waveform after the synthetic aperture processing should be evaluated numerically in order to calculate its maximum value and infer the expected peak signal to noise ratio. By considering a receiver noise figure and radio frequency losses of 4 dB respectively, atmospheric two way losses of 2 dB and a total antenna efficiency of 0.5 the resulting SNR for various backscattering coefficients are shown in figure 4. These curves are referred to a transmitted energy of 0.32 mJ which corresponds to a minimum pulse transmitted power of 8 Watt over a 40 μsec pulse.

With respect to the single pulse received waveform, a Brown-like echo⁹ is expected, since the system is operating in pulse-limited condition. In this case the peak value of the averaged return power can be evaluated analytically and it can be used to calculate the expected peak signal to noise ratio:

$$SNR = \frac{1}{4} \sqrt{\frac{\pi}{\log 2} \frac{E \lambda^2 G_0^2}{b \pi G_h^3} \frac{\sigma^0}{\sigma_0} \frac{\pi c}{B} \frac{1}{k T_0 F} \frac{1}{L_{RF} L_a}} \quad (7)$$

The signal to noise ratio as a function of the backscattering coefficient for various transmitted energy value is reported in figure 5 which shows that the system is able to assure good elevation estimates for a large interval of backscattering coefficient values with low transmitted energy (0.3÷0.5 mJ).

Operating frequency	13.8 GHz	Antenna dwell time	2.489 sec
S/C altitude	800 Km	Doppler bandwidth	13115 Hz
Parabolic Reflector Antenna Diameter	1.2 m	Burst length	4.668 msec
Real -3dB antenna aperture	1.33 deg	Number of pulses within the burst	88
Synthetic antenna aperture	17.9 mdeg	PRF	18853 Hz
Along-track resolution	250 m	BRI	11.139 msec
Integration time	4.668 msec	Spacing between burst	~ 83 m
Bandwidth	50 MHz	Reception length	6.471 msec
Vertical resolution	3 m	Pulse duration max	43 μsec
Across-track resolution	~ 4400 m	Number of looks	223

Table 2 - Design parameters for the Ku system.

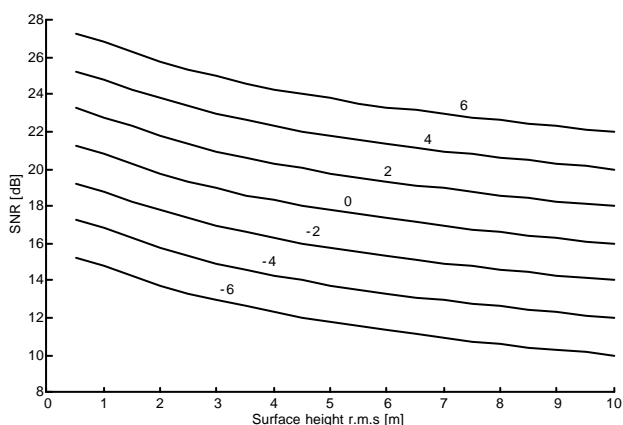


Figure 4 - Synthetic processing: signal to noise ratio vs surface height r.m.s. for various backscattering coefficient in dB assuming transmitted energy of 0.32 mJ.

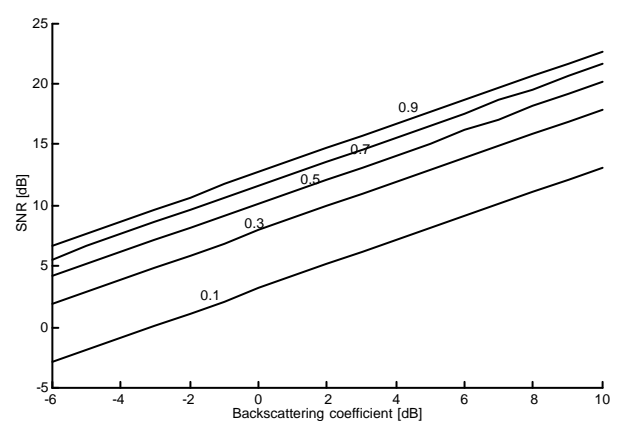


Figure 5 - Conventional altimetry: signal to noise ratio vs backscattering coefficient for various transmitted energy expressed in mJ.

As far as the expected correlation between pulses is concerned, by applying the Van Cittert-Zernike theorem¹⁰ it can be shown that a PRF value of about 2357 Hz is able to assure decorrelated echoes for any surface height r.m.s. Therefore, a pulse over eight should be considered in conventional altimetric processing which means that exactly 11 decorrelated pulses can be averaged during each burst.

3. INTERFEROMETRIC ALTIMETER

3.1 Review of the key concepts

SAR interferometry has shown to be one of the most promising techniques for deriving accurate and high resolution digital elevation models (DEM) of large areas. By using a couple of antennas separated by a distance B , it is in fact possible to derive the height of a target from the phase difference between the signals received by the two antennas. The relationship between the phase difference ($\Delta\Phi$) and the target's height (H) is very simple because it involves only geometric system parameters as shown by the (8), where a linearisation of the distance has been applied; R is the slant-range, θ is the off-nadir angle and B is the baseline between the two antennas as shown in figure 6:

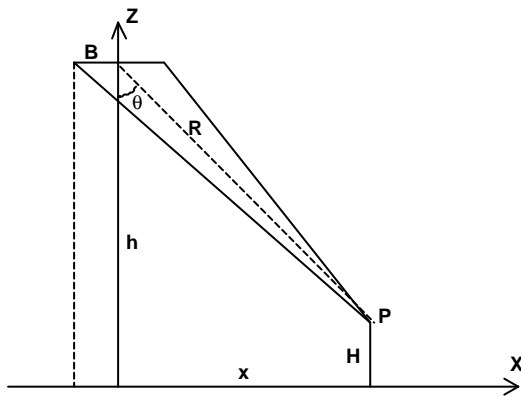


Figure 6 Interferometry observation geometry

$$H = h - R \cos \theta$$

$$\Delta\Phi \approx \frac{2\pi}{\lambda} B \sin \theta - \frac{B^2}{2R} \quad (8)$$

The steps required for obtaining a phase difference image (interferogram) useful to retrieve the surface height through the (8) consist of a synthetic aperture processing for each receiving channel, a data co-registration to compensate the different antennas point of view and a phase unwrapping. Each processing phase is quite critical from the point of view of time and hardware demand and, therefore, power in the order of some GFlops would need for real-time implementation. In particular the last operation of the phase unwrapping should be definitively avoided because completely automated and correct algorithms do not exist at present.

The accuracy attainable on the height estimate depends on the knowledge of the parameters involved in the (8) and on the various noise sources. Assuming independent parameters the accuracy on the final height estimate (σ_H) can be expressed as a function of the accuracies of spacecraft altitude (σ_h), range (σ_R), baseline length (σ_B) and phase difference ($\sigma_{\Delta\Phi}$), as:

$$\sigma_H^2 = \left(\frac{\partial H}{\partial h}\right)^2 \sigma_h^2 + \left(\frac{\partial H}{\partial R}\right)^2 \sigma_R^2 + \left(\frac{\partial H}{\partial B}\right)^2 \sigma_B^2 + \left(\frac{\partial H}{\partial \Delta\Phi}\right)^2 \sigma_{\Delta\Phi}^2 \quad (9)$$

Normally the first three terms are not critical because the uncertainty in the spacecraft altitude can introduce only a bias while both the range and baseline length are known with a high degree of accuracy. The knowledge of the baseline vector is a critical issue only for interferometry based on satellite multiple passes. Therefore, the most critical term is the phase noise which is generated by two mechanisms: the first one is due to temporal changes of the electromagnetic properties of the imaged scene while the second one is intrinsically caused by the speckle statistic and system transfer function. Dealing with systems based on contemporaneous observation, only the last phase noise component should be taken into account.

The variance of the phase difference can be evaluated numerically starting from the theoretical formulation of the probability distribution function which is known in the more general context of second order speckle statistics¹⁰. The probability density functions are always distributed around zero and sharpen for increasing values of the correlation coefficient γ . The phase difference variance is, therefore, a decreasing function of correlation coefficient.

The coherence depends either on the characteristics of the system transfer function and the statistical properties of the surface. With some assumptions it is possible to get the following analytical expression⁸ of this parameter as a function of main system parameters:

$$|\gamma| \approx \frac{M}{\lambda} \frac{B \rho_R}{b - H \sin \vartheta} \frac{1}{B + \text{SNR}^{-1}} \quad (10)$$

where ρ_R is the slant-range resolution. Finally, the multiplicative term of the phase variance in (9) can be easily computed by differentiating the (8) as:

$$\frac{\partial H}{\partial \Delta \Phi} = \frac{\partial H}{\partial \vartheta} \frac{\partial \vartheta}{\partial \Delta \Phi} = \frac{b - H \sin \vartheta}{2 \pi B} \frac{\sin \vartheta}{\cos^2 \vartheta} \quad (11)$$

Therefore, the attainable accuracy in the determination of surface elevation through interferometric systems can be greatly increased by decreasing the off-nadir angle ϑ . This basic property is the main reason for justifying the efforts in studying the feasibility and the performance of interferometric configuration with low off-nadir angle.

3.2 Near-nadir Interferometry

The main advantage of this kind of configuration has been analytically illustrated at the end of the previous paragraph and it consists in the high accuracy achievable in the determination of surface topography. The other advantages are concerned the simplifications that can be introduced in data processing. Firstly the registration of data received by the two antennas can be surely avoided since the expected translation in the cross-track direction mostly depends on the component of the baseline along the slant range direction, which is a decreasing function of the off-nadir angle. Secondly, the condition for avoiding the perils of the phase-unwrapping can be easily met. In fact, only one interferometric fringe will be present within the swath if the total phase variation is less than 2π , that is to say:

$$\sin \vartheta_{\max} - \sin \vartheta_{\min} \leq \frac{\lambda}{B} \quad (12)$$

being ϑ_{\min} and ϑ_{\max} the minimum and maximum observation angles for the selected observation geometry.

The last expression can easily be re-written as a function of the system cross-track swath, which can be maintained within the antenna aperture in elevation only if the baseline is comparable with the antenna dimension. This can compromise the feasibility of the system, but some margin can be gained at the expense of visible across-track swath and signal to noise ratio.

If either the registration and phase unwrapping are avoided with an appropriate choice of system parameters, the needed data processing will result very simplified and, therefore, suitable even for an on board implementation. Some problems can arise during the final step of slant to cross-track conversion. In fact, after the interferogram formation, by applying the (8), the processing is able to obtain a set of couples slant-range and height (R,H) or, equivalently, slant-range and off-nadir angle (R, ϑ). In order to obtain the final surface height image in across-track coordinate, each (R,H) couple should be mapped in the corresponding across-track and height couple. Unfortunately, the mapping law is intrinsically ambiguous and, therefore, a criterion for deriving a single height information for each across-track resolution cell should be adopted.

In addition, whatever the criterion is, the basic assumption is that all the points mapped in the same cross-track resolution cell are "good" in the sense that they are characterised by a phase difference directly related to the actual target height. The last condition is not verified when a layover occurs, i.e. when scattering cells at different height and across-track position are

mapped in the same slant range. In this case the signals returning from each scatterer are summed up coherently such as the resulting phase is definitely corrupted and the power is much higher than the mean one. If these points are not eliminated, they can affect negatively the height estimate in accordance with the chosen criterion of selection. To this end a suitable method could consist in the exploitation of the high power associated with such points.

3.3 Signal to noise ratio

In the previous paragraphs, the signal to noise ratio has been evaluated by considering analytical models based on Gaussian distributed topography. This basic assumption is no longer valid for the present system aimed to land/ice topography retrieval. Therefore, the expected signal to noise ratio can be evaluated by leaving out the effect of surface height distribution and by considering only the power received from an elementary resolution cell with the improvement given by the number of pulses integrated N_p and the modulation along the swath introduced by the antenna pattern, supposed Gaussian. The following expression can be obtained:

$$SNR = \frac{E_p \rho_x \rho_y N_p b_a A g}{4\pi \lambda^2 R^4} \frac{1}{\sigma_0} \frac{1}{KT_0 F} \frac{1}{L_a L_{RF}} \frac{\exp \left[\frac{M}{N} \log 2 \frac{\sin^2 \vartheta - \vartheta_0}{\sin^2 \vartheta_3 / 2} \right]}{\sin \vartheta} \quad (13)$$

where ρ_x is the along-track resolution, ϑ_3 and ϑ_0 are the -3 dB aperture in the elevation and the pointing angle of the antenna of area A. From the last expression it is evident that the minimum value of the signal to noise ratio occurs at the end of the swath, i.e. in correspondence with the maximum off-nadir angle.

3.4 System design

The interferometric system design will start from the parameters already set for the Ku synthetic aperture radar altimeter previously studied. The evaluation of the system baseline and off-nadir angle can be performed by taking into account the following considerations: a) the error in the height reconstruction by means of interferometry is an increasing function of the off-nadir angle through the multiplicative term in (11); the interferometric phase variance is, instead, a decreasing function of the correlation coefficient which, in turn, is an increasing function of either the off-nadir angle and the signal to noise ratio; b) the signal to noise ratio can be increased maintaining low the attenuation introduced by the antenna pattern within the swath and by decreasing the off-nadir angle; c) the baseline is mainly controlled by the condition (12) and its value should be the greatest possible since it can affect positively both the correlation coefficient and the multiplicative factor.

Starting from the definition of the slant range swath, a value 128 times the system resolution, i.e. 384 meters has been considered since the on-board processing is based on a FFT. Moreover, the cross-track swath can be approximately expressed as a function only of the minimum off-nadir angle which should not assume values too low in order to ensure a high attenuation of the nadir returns. Therefore, a value of 1.3 degrees equal to a -3dB antenna aperture has been selected. With this value a significantly large (more than 12 Km) cross-track swath can be achieved. The value of the maximum off-nadir angle can be easily determined by using a simple geometrical relation involving either the minimum off-nadir angle and slant-range values.

The choice of the baseline should be performed according to the (12) which can be rewritten in (14) as a function of a safety factor $\alpha < 1$ which should account for the expected surface topography (ΔH) within the swath and, mainly, the satellite orbit (Δh) variations, in order to assure in any case the formation of a single interferometric fringe. Table 3 summarises the system parameter obtained by considering a maximum orbit and topography variation of 25 Km and 1 Km respectively.

$$\vartheta_{\max} = \alpha \sin \left[\frac{B}{H} \frac{\lambda}{B} + \sin \vartheta_{\min} \right] \quad (14)$$

By using the obtained geometrical parameters, the (14) allows to evaluate the signal to noise ratio. Figure 7 shows its behaviour within the swath for a reference backscattering coefficient value of 0 dB and for a peak transmitted energy of 100

Watt. The signal to noise ratio can be used to estimate the correlation coefficient through (10) which, in turn, allows to estimate the phase difference variance by numerically integrating the theoretical probability density function of the phase difference. Finally the multiplicative factor of (11) can be evaluated and the expected height accuracy estimated by considering the improvement given by the number of looks integrated. The result is plotted in figure 8.

The rather constraining value of the baseline, only few centimeters greater than the antenna diameter, can be overcome by increasing a little bit the minimum off-nadir angle at the expense of the across-track swath, but maintaining nearly the same performances. A baseline of 1.3 m can be reached with a minimum and a maximum off-nadir angles of 1.5 and 2.32 degrees respectively and a cross-track swath of 11.5 Km.

The possibility of improving the system performance by increasing the antenna dimension has also been investigated. Unfortunately this action causes an increase of the minimum off-nadir angle too, since the (14) would entail a baseline value not feasible. In addition, by changing the antenna aperture, a new design of the whole synthetic aperture system is required. Only modest improvements (~10 cm) in the final height accuracy have been experienced.

Across-track swath	12.6 Km	Minimum off-nadir angle	1.3 deg
Antenna dimension	1.2 m	Maximum off-nadir angle	2.200 deg
Antenna -3dB beamwidth	1.3 deg	Pointing angle	1.75 deg
Safety factor	0.856	Baseline	1.23 m

Table 3 - Main geometrical parameters for the Ku interferometric system.

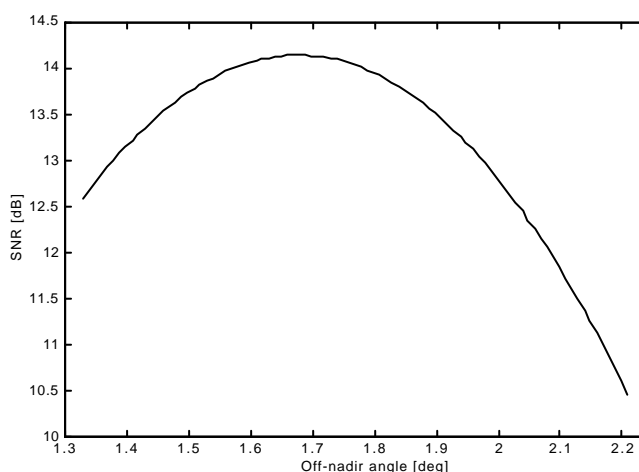


Figure 7 - System signal to noise ratio as a function of the off-nadir angle within the observable swath. with a backscattering coefficient of 0 dB and a peak transmitted energy of 100 Watt.

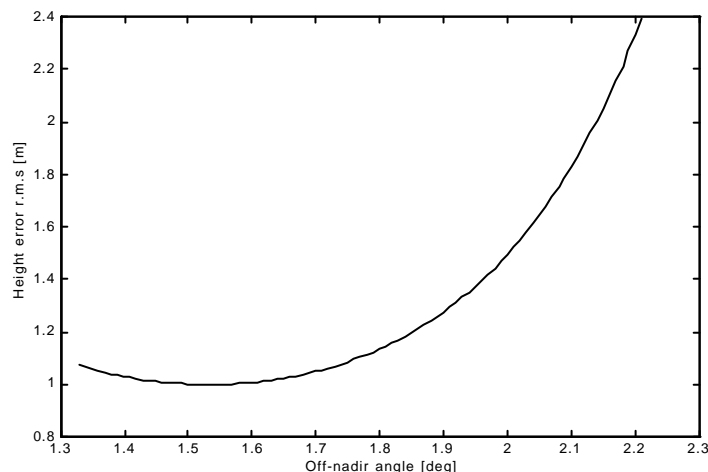


Figure 8 - Height root mean square error as a function of the off-nadir angle within the observable swath with a backscattering coefficient of 0 dB and a peak transmitted energy of 100 Watt.

4. CONCLUSIONS

In preparation of future missions a growing interest is rising for the development of new concepts potentially able to enlarge the field of applications being so far covered by conventional pulse limited radar altimeters. Up to now in fact, in spite

of an extremely high range accuracy achievable over oceans, conventional pulse limited altimeters are unable to retrieve details over ice or land surfaces because of the rather coarse horizontal resolution.

For these reasons, a way to make radar altimeters suitable for ice and land topography also, would be extremely attractive so that the requirements of a global topography mission with a unique payload system could be met. In this light investigations carried out by Alenia Spazio in the frame of internal research activities as well as of ESA feasibility studies have led to the identification of potential solutions based on synthetic aperture processing and interferometry applied to radar altimeters.

Synthetic aperture processing in satellite altimetry has also been recognised by other authors as a practical solution for the resolution enhancing in the direction of satellite motion. Such a technique has been applied to a Ka band as well as to a Ku band nadir looking altimeter. The Ka band option, in conjunction with a large antenna in the direction orthogonal to the satellite motion, allows to improve the resolution in across-track otherwise limited to the pulse limited footprint of conventional altimetric systems derived from ERS or RA-2 designs. Such a system could also be equipped with antenna beam steering capability in the across-track direction to achieve some swath coverage.

Application of synthetic aperture processing to a Ku band system derived from ERS or RA-2 leads instead to a really cost effective payload concept even if limited in across-track resolution performance. Such a system can however be regarded as the building block for a more powerful system relying on joint use of synthetic aperture and interferometric processing through a double antenna receiving subsystem.

The key feature of the interferometric altimeter concept developed by Alenia Spazio is its innovative measurement technique which is based on interferometry at very low off-nadir angles. The height measurement is retrieved looking at the phase difference between two collected images but no phase unwrapping is required: the system geometry is in fact such that a unique interference fringe is generated within the observed swath. Height accuracy for this system has been evaluated and looks extremely promising: figures in the order of 1 meter can in fact be achieved. Furthermore, the system is fully compatible with conventional altimetry: a unique payload providing conventional pulse limited altimetry, synthetic aperture nadir looking altimetry and near sub-nadir synthetic aperture/interferometric altimetry can thus be conceived with a minimum level of complexity added to the original design of conventional altimetric systems. Various types of altimetric products can consequently be obtained to satisfy the science needs.

5. REFERENCES

1. Provvedi, C. Zelli, A. Resti, S. Idler, "RA-2 Radar Altimeter: Instrument Operation Concept and System Performance" *IAF Congress 1995*
2. L. Parson and E. J. Walsh, "Off-nadir radar altimetry" *IEEE Transaction on Geoscience and Remote Sensing*, Vol. 27, no. 2, March 1989.
3. R. Jensen, "Design and performance analysis of a phase-monopulse radar altimeter for continental ice sheet measurement" *IGARSS 1995 Proceedings*
4. K. Raney, "A delay/Doppler radar altimeter for ice sheet monitoring", *IGARSS 1995 Proceedings*.
5. K. Raney, "A down-looking satellite SAR with on-board real time-rate processing: the delay/Doppler radar altimeter" *EUSAR'96 proceeding*, Königswinter, Germany 1996.
6. Elachi, K. E. Im, F. Li and E. Rodriguez, "Global digital topography mapping with synthetic aperture scanning radar altimeter" *Int. J. Remote Sensing*, 1990, Vol. II, no. 4, pp. 585-601.
7. Barbarossa, G. Picardi, "The Synthetic Aperture Concept applied to the Altimetry: Surface and Subsurface Imaging" *Proceedings of Consultative Meeting on Imaging Altimeter Requirements and Techniques MSSL 30 May - 1 June 1990*.
8. Rodriguez, E., Martin, J. M., "Theory and design of interferometric synthetic aperture radars" *IEE Proceedings*, Vol. 139, No. 2, April 1992, pp. 147-159.
9. Gary S. Brown, "The average impulse response of a rough surface and its applications" *IEEE Transactions on Antennas and Propagation*, January 1977, pp. 67-74

10. W. Goodman, *Laser speckle and related phenomena*, J. C. Dainty (Ed.), Springer & Verlag, 1975.